Published in final edited form as:
Nat Cell Biol. 2006 December ; 8(12): 1407–1414. doi:10.1038/ncb1506.

A novel function of *Drosophila* eIF4A as a negative regulator of Dpp/BMP signalling that mediates SMAD degradation

Jinghong Li[1] and **Willis X. Li**[1,2]

[1] Department of Biomedical Genetics, University of Rochester Medical Center, Rochester, NY 14642, USA

Abstract

Signalling by the TGF-β superfamily member and BMP orthologue Decapentaplegic (Dpp) is crucial for multiple developmental programmes and has to be tightly regulated. Here, we demonstrate that the *Drosophila* Dpp pathway is negatively regulated by eukaryotic translation initiation factor 4A (eIF4A), which mediates activation-dependent degradation of the Dpp signalling components Mad and Medea. *eIF4A* mutants exhibit increased Dpp signalling and accumulation of Mad and phospho-Mad. Overexpression of eIF4A decreases Dpp signalling and causes loss of Mad and phospho-Mad. Furthermore, eIF4A physically associates with Mad and Medea, and promotes their degradation following activation of Dpp signalling in a translation-independent manner. Finally, we show that eIF4A acts synergistically with, but independently of, the ubiquitin ligase DSmurf, indicating that a dual system controls SMAD degradation. Thus, in addition to being an obligatory component of the cap-dependent translation initiation complex, eIF4A has a novel function as a specific inhibitor of Dpp signalling that mediates the degradation of SMAD homologues.

To understand the regulation of Dpp signalling, we have previously identified a dominant-negative mutation in eukaryotic translation initiation factor 4A (eIF4A), which acts as a suppressor of *dpp* haploinsufficiency[1]. This allele, $eIF4A^{R321H}$ (also known as $eIF4A^{YE9}$), is associated with an increased number of amnioserosa cells[1], the fate of which is determined by Dpp in the early *Drosophila* embryo[2]. To investigate whether *eIF4A* mutations cause increased Dpp signalling in general, we examined the effects of *eIF4A* mutations on Dpp signalling in other developmental or genetic contexts. First, we found that $eIF4A^{R321H}$ and $eIF4A^{1006}$ (a null allele[1,3]) dominantly suppressed the sterility of females that were doubly heterozygous for null mutations of *Mad* and *saxophone* (*sax*) (see Methods), which encode homologues of mammalian Smad1/5/8 and type I activin receptor, respectively[4–8]. Embryos that are produced by $Mad\ sax^1$/+ female flies die with a partially ventralized phenotype (data not shown; also see refs 5, 6). In contrast, $Mad\ sax^1/eIF4A^{R321H}$ and $Mad\ sax^1/eIF4A^{1006}$ females laid morphologically normal eggs that hatched to viable adult progeny (Table 1), indicating that reducing the amount of *eIF4A* can compensate for a reduced maternal *Mad* and *sax* dosage for embryonic viability. Second, $eIF4A^{R321H}$ and $eIF4A^{1006}$ dominantly

[2]Correspondence should be addressed to W.X.L. (willis_li@urmc.rochester.edu).

AUTHOR CONTRIBUTIONS

J.L. coplanned the project, performed experiments and analysed data. W.X.L. planned the project and wrote the paper.

COMPETING FINANCIAL INTERESTS

The authors declare that they have no competing financial interests.

Note: Supplementary Information is available on the Nature Cell Biology website.

suppressed the partial lethality and 'thick vein' phenotype that was associated with reduced levels of the type I receptor Thickveins[6,9] (Fig. 1a; Table 1), indicating that the effect of *eIF4A* mutations on Dpp signalling is not limited to embryogenesis. Third, transient ectopic expression of *dpp* induced by mild heat shock was tolerated in wild-type flies, but resulted in lethality in a $eIF4A^{R321H}$/+ background, indicating that $eIF4A^{R321H}$ dominantly enhances the effects of *dpp* ectopic expression (Table 1). $eIF4A^{R321H}$ heterozygosity similarly enhanced the effects of overepxressing *dpp* by the eye-specific *GMR–Gal4* (see below and Fig. 1h). Therefore, *eIF4A* mutations seem to augment the Dpp signalling strength.

To investigate at which step loss of eIF4A increases Dpp signalling, we examined the levels of active or phosphorylated Mad (pMad). In early wild-type embryos, pMad signals are detected in spatial and temporal patterns that are correlated with *dpp* expression[10]. At stage 10, pMad signals had dissipated from the procephalon and posterior midgut of wild-type embryos (Fig. 1b; also see refs 10, 11), but were still detected in $eIF4A^{R321H}$ embryos (Fig. 1b) — a phenotype that is very similar to that caused by loss of DSmurf[11] — indicating a prolonged duration of Dpp signalling. Pronounced elevation and expansion of pMad signals were also detected in stage 11 (see Supplementary Information, Fig. S1) and stage 13 $eIF4A^{R321H}$ embryos (Fig. 1c). Consistent with the higher levels and expanded domains of pMad signals, we found that *dpp* expression in gc and ps7, which is subject to positive autoregulation, was also expanded in $eIF4A^{R321H}$ embryos (Fig. 1d). As we detected expanded domains but little or no ectopic pMad, and the initial pattern of *dpp* or pMad at stages 5–6 was not obviously changed in $eIF4A^{R321H}$ embryos (data not shown; see Supplementary Information, Fig. S1), the presence of higher levels and expanded domains of pMad signals in later embryonic stages indicate a prolonged Mad activation in $eIF4A^{R321H}$ embryos.

To understand the cause of the prolonged Mad activation, we examined Mad protein levels in $eIF4A^{R321H}$ embryos. Mad protein levels are generally low in all tissues, including ps7, in wild-type embryos (Fig. 1e; left). However, in $eIF4A^{R321H}$ embryos, elevated levels of Mad protein were found in ps7 (Fig. 1e; right). The observed accumulation of Mad protein is consistent with the idea that Mad protein levels are normally negatively controlled by protein degradation, and *eIF4A* mutations disrupt this process. Interestingly, the higher levels of Mad protein that were detected in $eIF4A^{R321H}$ embryos seemed to be nuclear localized, indicating that $eIF4A^{R321H}$ may interfere with the degradation of activated Mad.

To investigate whether *eIF4A* mutant cells autonomously increase Mad phosphorylation and protein levels, we generated cell clones that were mutant for a weak allele of *eIF4A*, $eIF4A^{1069}$, as cells that are mutant for strong *eIF4A* alleles are not viable[3]. We examined multiple larval tissues and found increased pMad and Mad levels associated with $eIF4A^{1069}$ mutant clones, most prominently in the presumptive adult gut (Fig. 1f, g). These results indicate that *eIF4A* mutations cause prolonged Mad phosphorylation, which might be due to reduced Mad degradation.

To test whether wild-type eIF4A antagonizes Dpp signalling, we expressed *eIF4A* using the Gal4/UAS system[12]. First, expressing one copy of *UAS–eIF4A* by the eye-specific *GMR–Gal4*, which by itself had little effects, completely neutralized the effects of ectopic *dpp* expression on eye development (Fig. 1h), indicating that overexpression of eIF4A antagonizes Dpp signalling. Conversely, expressing *dpp* by *GMR–Gal4* in $eIF4A^{R321H}$ heterozygotes caused lethality, and the escapers had enlarged and deformed eyes (Fig. 1h), which is consistent with the idea that endogenous eIF4A antagonizes Dpp signalling. Second, expressing *eIF4A* by the wing-margin-specific *C96–Gal4* resulted in 'notches' in the wing margin (Fig. 1i; right) — a phenotype that is similar to those produced by expressing dominant-negative molecules of the Dpp pathway, such as Put and Sax (Fig. 1i;

middle). We examined pMad levels in 3rd instar imaginal discs and found a prominent loss of pMad signals in wing-margin primordial cells in which *C96–Gal4* is expressed (Fig. 1j). These results are consistent with the notion that wild-type eIF4A negatively modulates Dpp signalling at the level of Mad protein regulation.

To investigate the molecular mechanism by which eIF4A negatively modulates Dpp signalling, we co-expressed Mad, Medea and $eIF4A^{WT}$ (or $eIF4A^{R321H}$) in 293T cells with or without the activated form of Dpp receptor Tkv^{QD}, which is able to phosphorylate and activate Mad in a ligand-independent manner[13]. Medea is a co-Smad that is homologous to Smad4 (refs 14, 15). It has been reported that transfected Mad and Medea are localized in the cytoplasm, and cotransfection with Tkv^{QD} results in their nuclear translocation[15]. We found that, in the absence of Tkv^{QD}, $eIF4A^{WT}$ (or $eIF4A^{R321H}$) and Mad were localized in the cytoplasm in the same nonuniform patterns (Fig. 2a, rows 1, 3). However, following co-transfection with Tkv^{QD}, in cells transfected with $eIF4A^{WT}$, the levels of Mad were reduced and its nuclear translocation was not detectable (Fig. 2a, row 2). This is in contrast to cells without transfected eIF4A (see Supplementary Information, Fig. S2; also see ref. 15) or to those transfected with $eIF4A^{R321H}$ (Fig. 2a, row 4), which exhibit prominent Mad nuclear translocation. These results are consistent with the notion that $eIF4A^{WT}$ antagonizes and $eIF4A^{R321H}$ enhances Dpp signalling.

As transfected eIF4A and Mad both reside in the cytoplasm in similar patterns prior to Mad activation, we tested whether they physically interact with the following assays. First, in co-transfected 293T cells, we found that eIF4A was able to co-immunoprecipitate with either Mad or Medea (Fig. 2b), indicating that eIF4A physically interacts with both Mad and Medea in transfected cells. Second, we performed immunoprecipitation studies using embryo extracts, and found that $eIF4A^{WT}$ and, to a lesser extent, $eIF4A^{R321H}$ were co-immunoprecipitated with Mad from embryo extracts (Fig. 2c). Finally, we confirmed the physical interaction between Mad and eIF4A using bacterially expressed eIF4A protein fragments and embryo lysate. The results indicated that Mad binds to the full-length eIF4A (Fig. 2d, lane 6) mainly through the carboxyl terminus (Fig. 2d, lane 4), and has a lower affinity for the amino terminus or $eIF4A^{R321H}$ (Fig. 2d, lanes 5, 7). These results indicate that $eIF4A^{WT}$ is able to physically associate with Mad and that $eIF4A^{R321H}$ is less able to do so.

We next examined the protein levels of Mad and Medea in the presence or absence of eIF4A and/or Dpp signalling in transfected cells. We found that low levels of Dpp signalling (low concentration of Tkv^{QD}) induced a dramatic degradation of Mad and Medea, as well as eIF4A itself, in the presence of $eIF4A^{WT}$ (Fig. 3a, lane 6) but not $eIF4A^{R321H}$ (Fig. 3a, lane 7), or in the absence of Tkv^{QD} (Fig. 3a, lane 3). We further confirmed that eIF4A-induced Mad and Medea degradation depends on the dosage of Tkv^{QD} and the proteosome system. Degradation of Mad and Medea was detected in the absence of exogenous eIF4A at high doses but not low doses of Tkv^{QD} (Fig. 3b, lanes 2, 3). However, the presence of exogenous $eIF4A^{WT}$ or, to a lesser extent, $eIF4A^{R321H}$ resulted in the disappearance of Mad and Medea even at low doses of Tkv^{QD} (Fig. 3b, lanes 4, 6), and this effect was inhibited by the proteosome inhibitor MG-132 (Fig. 3b, lane 8), indicating that eIF4A promotes proteosome-dependent degradation of both Mad and Medea.

It has been shown that Mad is ubiquitinated prior to its degradation[16]. We found that eIF4A increased Dpp signal-dependent (+Tkv^{QD}) ubiquitination of Mad (Fig. 3c). Moreover, we found that eIF4A itself also appeared to be ubiquitinated and degraded following activation of Dpp signalling, as Tkv^{QD} caused a dramatic increase in eIF4A ubiquitination and degradation only in the presence of Mad and Medea, but not in their absence (Fig. 3d; compare lanes 2 and 4).

As the known function of eIF4A has been in translation initiation, it is formally possible that eIF4A might preferentially promote the translation of an inhibitor of the Dpp pathway. However, this is unlikely to be the case based on the following observations. First, when overexpressed in cultured cells, eIF4A^{R321H} also promoted Mad and Medea degradation especially at high doses of Dpp signalling, albeit less efficiently than eIF4A^{WT} (see Fig. 3b). This is presumably due to its ability to bind to Mad and Medea (see Fig. 2b–d) and to be ubiquitinated (see Fig. 3d). However, eIF4A^{R321H} behaves genetically as a dominant-negative molecule in causing lethality and growth delay[1], possibly by inhibiting general translation. Indeed, purified eIF4A^{R321H} protein potently inhibited protein translation in an *in vitro* system in a dose-dependent manner (see Supplementary Information, Fig. S3a). These results indicate that the ability of eIF4A to inhibit Dpp signalling is separable from its function as a translation initiation factor. Second, inhibiting the eIF4F complex does not lead to increased Dpp signalling. Mutations in *eIF4E* cause lethality and larval growth delay[17], phenotypes that are essentially identical to those of *eIF4A*. eIF4E is an essential regulatory subunit of the eIF4F complex[17]. However, none of the *eIF4E* mutants we tested caused increased Dpp signalling in a sensitized assay (see below and Fig. 4a; data not shown). We further examined the number of amnioserosa cells, which reflects the levels of Dpp signalling in the early embryo[1,2]. Unlike *eIF4A* or other *Su(dpp)* mutations[1], *eIF4E* mutant embryos had a normal number of amnioserosa cells (see Supplementary Information, Fig. S3c). These results indicate that the negative modulation of Dpp signalling by eIF4A is independent of its function in protein translation.

The ubiquitin E3 ligase DSmurf (encoded by *lack*) has been shown to negatively regulate Dpp signalling[11] by specifically binding to and promoting degradation of phospho-Mad[16]. To investigate whether the function of eIF4A in mediating Mad degradation depends on DSmurf, we tested genetic interactions and the epistatic relationship between *eIF4A* and *DSmurf* mutations in a sensitized genetic assay. Flies with one copy and three copies of dpp^+ (1xdpp^+ and 3xdpp^+, respectively) are inversely sensitive to maternal-effect mutations that increase Dpp signalling strength[1,5,6]. Increasing Dpp signalling promotes the viability of 1xdpp^+ animals, which are normally not viable in an otherwise wild-type genetic background[1,5,6], and decreases that of 3xdpp^+ animals. Thus, when fathered by 0xdpp^+/2xdpp^+ males (see Methods), the ratio of F1 siblings inheriting 1xdpp^+ versus 3xdpp^+ is a sensitive measurement of the effects of genetic mutations carried by the mother on Dpp signalling.

This sensitized assay allowed us to make the following two findings with regards to eIF4A. First, we found that *eIF4A* and *DSmurf* mutations interact synergistically in trans-heterozygotes. Heterozygous mutations in *eIF4A* and *DSmurf* individually either did not rescue or moderately rescued the lethality of 1xdpp^+ animals, such that when females that were heterozygous for $eIF4A^{1006}$, $eIF4A^{R321H}$ or $lack^{KG07014}$ (a strong allele) were mated to 0xdpp^+/2xdpp^+ males, the ratios of 1xdpp^+ versus 3xdpp^+ progeny in the F1 were 0 (no rescue), 0.15 and 0.29, respectively (Fig. 4a). However, transheterozygosity of *eIF4A* and *DSmurf* mutations produced synergistic effects on the viability of F1 progeny, dramatically increasing the number of 1xdpp^+ offspring at the expense of their 3xdpp^+ siblings, resulting in ratios of 1.2 and 1.4, respectively (Fig. 4a). Generally increasing Dpp signalling did not result in synergistic interaction with *DSmurf*. Specifically, low-level expression of the activative Tkv^{QD} molecule (using *hs–Gal4/UAS–Tkv^{QD}* females under mild heat-shock conditions) can suppress *dpp* haplo-lethality, resulting in a 1xdpp^+ versus 3xdpp^+ progeny ratio 0.01 (8/896). This is significant because 1xdpp^+ survivors were never found in the progeny of wild-type females ($n > 5000$) or $eIF4A^{1006}$/+ females ($n > 2000$). However, in the progeny of $lack^{KG07014}$/+;*hs–Gal4/UAS–Tkv^{QD}* females, the ratio was not significantly different from that of $lack^{KG07014}$/+ females (Fig. 4a). Taken together with previous

results[16,11], the synergy between eIF4A and DSmurf strongly indicates that they function in the same biological process — that is, promoting Mad protein degradation.

Second, we tested whether the effects of *eIF4A* mutations on Dpp signalling depend on DSmurf. Flies without DSmurf (*lack*^{KG07014}*/Df*) were viable and fertile, and the females produced progeny in which the ratio of 1x*dpp*$^{+}$ versus 3x*dpp*$^{+}$ animals was >1.5 (Fig. 4a). However, animals with a half dose of *eIF4A*$^{+}$ in this genetic background (*eIF4A*^{1006}/+;*lack*^{KG07014}/Df), although perfectly viable, resulted in complete lethality of 3x*dpp*$^{+}$ offspring (ratio = 8; Fig. 4a). Flies heterozygous for *eIF4A*^{R321H} in the absence of DSmurf (*eIF4A*^{R321H}/+;*lack*^{KG07014}*/Df*) were barely viable (10.5% viable; *n* = 228) and completely sterile, whereas either *eIF4A*^{R321H}/+ or *lack*^{KG07014}*/Df* flies separately were perfectly viable and fertile (data not shown). Thus, *eIF4A* mutations further enhance the mutant phenotypes of flies without DSmurf.

To further substantiate this finding, we examined *eIF4A* embryos lacking both maternal and zygotic DSmurf. Increased Dpp signalling can lead to expansion of dorsal/lateral cell fates at the expense of ventral cell fates. We found that although embryos produced by either *eIF4A*^{1006}/+ or *lack*^{KG07014}*/Df* females (crossed to *lack*^{KG07014}/Df males) exhibited no significant dorsalization, those from *eIF4A*^{1006}/+;*lack*^{KG07014}*/Df* females were moderately (yet significantly) dorsalized, and embryos from *eIF4A*^{R321H}/+;*lack*^{KG07014}*/Df* females were completely dorsalized (Fig. 4b). Consistent with these results, embryos from *eIF4A*^{1006}/+;*lack*^{KG07014}*/Df* females exhibit more pronounced Mad accumulation (Fig. 4c). Thus, reducing eIF4A can further increase Dpp signalling and Mad accumulation in the absence of DSmurf. These results indicate that eIF4A and DSmurf can function independently in controlling Mad degradation.

In conclusion, our results indicate that eIF4A plays an essential role in limiting the duration and spatial distribution of Dpp signalling by promoting Mad/Medea degradation. We propose that in the absence of Dpp signals, eIF4A is able to physically associate with both Mad and Medea. Following the activation of the Dpp pathway, eIF4A promotes the ubiquitination and degradation of Mad and Medea, leading to attenuation and termination of Dpp signalling. eIF4A may function as an adaptor that links SMAD proteins to a degradation system that can be independent of the ubiquitin ligase DSmurf. We found no evidence that eIF4A mutations affect the Hedgehog and Wingless signalling pathways by genetic interaction analyses (see Supplementary Information, Fig. S4), thus eIF4A seems to be a specific regulator of Dpp signalling.

METHODS

Fly stocks and genetics

All crosses were carried out at 25 °C on standard cornmeal/agar medium. *eIF4A*^{R321H} and transgenic flies carrying *UAS–eIF4A* and *UAS–eIF4A*^{R321H} were as described previously[1]. *UAS–Tkv*^{QD}, *UAS–Put*^{DN} and *UAS–Sax*^{DN} were as described previously[13,18]. The P-element-associated *eIF4A* alleles (*eIF4A*^{1069} and *eIF4A*^{1006}) were as described previously[3]. *Sp dppH* ^{46}*/CyO-23* flies have the 0x*dpp*$^{+}$/2x*dpp*$^{+}$ genotype, as they carry a *dpp* null mutation (0x*dpp*$^{+}$) and two doses of *dpp*$^{+}$ on the *CyO-23* balancer chromosome: the endogenous *dpp*$^{+}$ and a *p[dpp*$^{+}$*]* transgene, as previously described[1,5]. Crossing females (*dpp*$^{+}$/*dpp*$^{+}$) to *Sp dppH* ^{46}*/CyO-23* males produces 1x*dpp*$^{+}$ and 3x*dpp*$^{+}$ animals in the F1 progeny, allowing determination of their ratios. The *Mad sax* double-mutant stock *Df(2L)JS17 sax*^{1}*/CyO-23* is as described previously[5]. *Df(2L)JS17* is a deficiency that removes *Mad*, thus was used as a null allele of *Mad*. Somatic mutant clones for *tkv*^{4} and *eIF4A*^{1069} were generated using the FLP–FRT method by crossing *FRT*^{40A} *tkv*^{4}*/CyO* or *FRT*^{40A} *eIF4A*^{1069}*/CyO* flies to *hs–flp;FRT*^{40A} or *hs–Myc* [Au: OK?], respectively. The

resulting larvae were heat-shocked for 2 h at 37 °C during the 2nd and early 3rd instar larval stages and dissected at the late 3rd instar stage. A brief heat-shock was administered 15 min before dissection to increase *hs–Myc* expression for marking the clones. All other stocks, including *DSmurf* mutants (*lack*^{KG07014} and *Df(2R)Exel7149*), *eIF4A–lacZ* and *dpp–lacZ* enhancer traps (*eIF4A*^{k01501}, *eIF4A*^{02439} and *dpp*^{P10638}), and various tissue-specific *Gal4* lines, including *C96–Gal4* (ref. 19), *hs–Gal4*, *GMR–Gal4* and *UAS–dpp* were from public *Drosophila* stock centres or as described previously[1]. *lack*^{KG07014} seemed to be a stronger allele than the reported null allele *lack*^{15C} (ref. 11), based on the observation that, when mated to *dppH* ^{46}*/CyO-23* males, *lack*^{KG07014}/+ mothers produced 25% viable 1x*dpp*$^{+}$ progeny, whereas <3% 1x*dpp*$^{+}$ animals survived from *lack*^{15C}/+ mothers (also see ref. 11).

Plasmids and antibodies

His-tagged full-length and N- and C-terminal eIF4A constructs were made by ligating PCR-amplified eIF4A or eIF4A^{R321H} cDNA fragments[1] to pQE vectors (Stratagene, La Jolla, CA) and subsequently subcloned into pcDNA3 (Invitrogen, Carlsbsd, CA). PCR primers for eIF4A-N and eIF4A-C were cgatGAGCTCggatgaccgaaatgagata (forward) and cgcaTCTAGAtaa tgggggcagcatcttgaa (reverse), and ctatGAGCTCtttcaagatgctgccccca (forward) and cgcaTCTAGAgcggctcagcagaaaaaa (reverse), respectively. The R321H substitution was located in the C terminus. Flag–Mad, Myc–Medea and TKV^{QD} constructs (generous gifts from M. Kawabata) were as described previously[20].

The primary antibodies (dilutions) used for whole-mount immunostaining and western blots were: rabbit anti-eIF4A (a gift from P. Lasko, McGill University, Canada; 1:300), sheep anti-eIF4A-c (a gift from C. Proud, University of British Columbia, Canada; 1:300), rabbit anti-pMad (PS1; a gift from P. ten Dijke, The Netherlands Cancer Institute, The Netherlands; 1:100), mouse anti-Myc (9E10; Developmental Hybridoma Bank, Iowa City, IA; 1:50), anti-Flag (M2; Sigma, St Louis, MO; 1:1000), mouse anti-β-gal (Promega, Madison, WI; 1:1000), goat anti-Mad (Santa Cruz, Santa Cruz, CA; 1:250) and anti-polyhistidine (Sigma; 1:2000). Different fluorophore-conjugated secondary antibodies were obtained from Molecular Probes (Carlsbad, CA; 1:250). HRP-conjugated secondary antibodies (Promega; 1:1000) were used for western blots.

Cell culture and immunoprecipitation

293T cells were cultured in DMEM (Invitrogen) supplemented with 10% fetal bovine serum in six-well plates. Cells were transfected with appropriate expression plasmids using FuGene 6 (Roche, Basel, Switzerland) according to the manufacturer's instructions. Cells were harvested 48 h after transfection and were stained with the indicated antibodies or lysed in cell lysis buffer (20 mM Tris-HCl at pH 7.5, 150 mM NaCl, 1 mM Na_2EDTA, 1 mM EGTA, 1% Triton-X-100, 2.5 mM sodium pyrophosphate, 1 mM β-glycerophosphate, 1 mM Na_3VO_4, 1 μg ml^{-1} leupeptin) (Cell Signaling Technology, Danvers, MA) for immunoprecipitation or SDS–PAGE. For proteosome inhibition, MG-132 (Sigma) was added at 50 μM 4 h prior to lysis. To immunoprecipitate endogenous Mad or eIF4A, extracts from 200 *Drosophila* embryos (0–24 h old) of appropriate genotype were used.

Pull-down and *in vitro* translation assays

1 μg of bacterially expressed His-tagged eIF4A protein was incubated with 200 μl of embryo extracts (in cell lysis buffer; see above) and 20 μl of Ni-NTA agarose beads for 2 h at room temperature. The Ni-NTA agarose beads were spun down and washed in the same buffer and subjected to SDS–PAGE to analyze bound proteins by western blotting with anti-Mad and anti-eIF4A.

In vitro translation was performed using the TNT® T7 Coupled Reticulocyte Lysate System in conjunction with the Transcend™ Colorimetric Non-Radioactive Translation Detection System (Promega) as per the manufacturer's instructions. His-tagged eIF4A proteins expressed in *Escherichia coli* and quantified by SDS–PAGE, followed by Coomassie Blue staining, were included in the assays. The translation rate was measured by the amount of firefly luciferase (internal positive control provided by the Kit) produced, which had incorporated biotinylated lysine and was detected by the Colorimetric (BCIP/NBT) reagents following SDS–PAGE and transfer per the manufacturer's instructions.

Supplementary Material

Refer to Web version on PubMed Central for supplementary material.

Acknowledgments

We thank S. Matics for technical assistance, M. Kawabata, P. Lasko, P. ten Dijke, C. Proud, W. Gelbart, D. Bohmann, Y. Sun, J. Zhao, J. Jiang, C. Proschel, and the Bloomington *Drosophila* Stock Center for various reagents and *Drosophila* strains. We thank Y. Sun for insightful discussions regarding possible mechanisms of eIF4A involvement in Dpp signalling and comments on the manuscript. J.L. was a recipient of the Wilmot Cancer Research Fellowship from the James P. Wilmot Foundation. This study was supported, in part, by grants from the National Institutes of Health (R01GM65774; R01GM077046) and an American Cancer Society Research Scholar Grant (RSG-06-196-01-TBE) to W.X.L.

References

1. Li J, Li WX, Gelbart WM. A genetic screen for maternal-effect suppressors of decapentaplegic identifies the eukaryotic translation initiation factor 4A in *Drosophila*. Genetics. 2006; 171:1629–1641. [PubMed: 15972466]
2. Wharton KA, Ray RP, Gelbart WM. An activity gradient of decapentaplegic is necessary for the specification of dorsal pattern elements in the *Drosophila* embryo. Development. 1993; 117:807–822. [PubMed: 8330541]
3. Galloni M, Edgar BA. Cell-autonomous and non-autonomous growth-defective mutants of *Drosophila melanogaster*. Development. 1999; 126:2365–2375. [PubMed: 10225996]
4. Newfeld SJ, et al. Mothers against dpp participates in a DDP/TGF-β responsive serine-threonine kinase signal transduction cascade. Development. 1997; 124:3167–3176. [PubMed: 9272957]
5. Sekelsky JJ, Newfeld SJ, Raftery LA, Chartoff EH, Gelbart WM. Genetic characterization and cloning of mothers against dpp, a gene required for decapentaplegic function in *Drosophila melanogaster*. Genetics. 1995; 139:1347–1358. [PubMed: 7768443]
6. Brummel TJ, et al. Characterization and relationship of Dpp receptors encoded by the saxophone and thick veins genes in *Drosophila*. Cell. 1994; 78:251–261. [PubMed: 8044839]
7. Penton A, et al. Identification of two bone morphogenetic protein type I receptors in *Drosophila* and evidence that Brk25D is a decapentaplegic receptor. Cell. 1994; 78:239–250. [PubMed: 8044838]
8. Xie T, Finelli AL, Padgett RW. The *Drosophila* saxophone gene: a serine-threonine kinase receptor of the TGF-β superfamily. Science. 1994; 263:1756–1759. [PubMed: 8134837]
9. Nellen D, Affolter M, Basler K. Receptor serine/threonine kinases implicated in the control of *Drosophila* body pattern by decapentaplegic. Cell. 1994; 78:225–237. [PubMed: 8044837]
10. Dorfman R, Shilo BZ. Biphasic activation of the BMP pathway patterns the *Drosophila* embryonic dorsal region. Development. 2001; 128:965–972. [PubMed: 11222150]
11. Podos SD, Hanson KK, Wang YC, Ferguson EL. The DSmurf ubiquitin-protein ligase restricts BMP signaling spatially and temporally during *Drosophila* embryogenesis. Dev Cell. 2001; 1:567–578. [PubMed: 11703946]
12. Brand AH, Perrimon N. Targeted gene expression as a means of altering cell fates and generating dominant phenotypes. Development. 1993; 118:401–415. [PubMed: 8223268]
13. Nellen D, Burke R, Struhl G, Basler K. Direct and long-range action of a DPP morphogen gradient. Cell. 1996; 85:357–368. [PubMed: 8616891]

14. Hudson JB, Podos SD, Keith K, Simpson SL, Ferguson EL. The *Drosophila* Medea gene is required downstream of dpp and encodes a functional homolog of human Smad4. Development. 1998; 125:1407–1420. [PubMed: 9502722]

15. Wisotzkey RG, et al. Medea is a *Drosophila* Smad4 homolog that is differentially required to potentiate DPP responses. Development. 1998; 125:1433–1445. [PubMed: 9502724]

16. Liang YY, et al. dSmurf selectively degrades decapentaplegic-activated MAD, and its overexpression disrupts imaginal disc development. J Biol Chem. 2003; 278:26307–26310. [PubMed: 12754252]

17. Lachance PE, Miron M, Raught B, Sonenberg N, Lasko P. Phosphorylation of eukaryotic translation initiation factor 4E is critical for growth. Mol Cell Biol. 2002; 22:1656–1663. [PubMed: 11865045]

18. Haerry TE, Khalsa O, O'Connor MB, Wharton KA. Synergistic signaling by two BMP ligands through the SAX and TKV receptors controls wing growth and patterning in *Drosophila*. Development. 1998; 125:3977–3987. [PubMed: 9735359]

19. Gustafson K, Boulianne GL. Distinct expression patterns detected within individual tissues by the GAL4 enhancer trap technique. Genome. 1996; 39:174–182. [PubMed: 8851804]

20. Inoue H, et al. Interplay of signal mediators of decapentaplegic (Dpp): molecular characterization of mothers against dpp, Medea, and daughters against dpp. Mol Biol Cell. 1998; 9:2145–2156. [PubMed: 9693372]

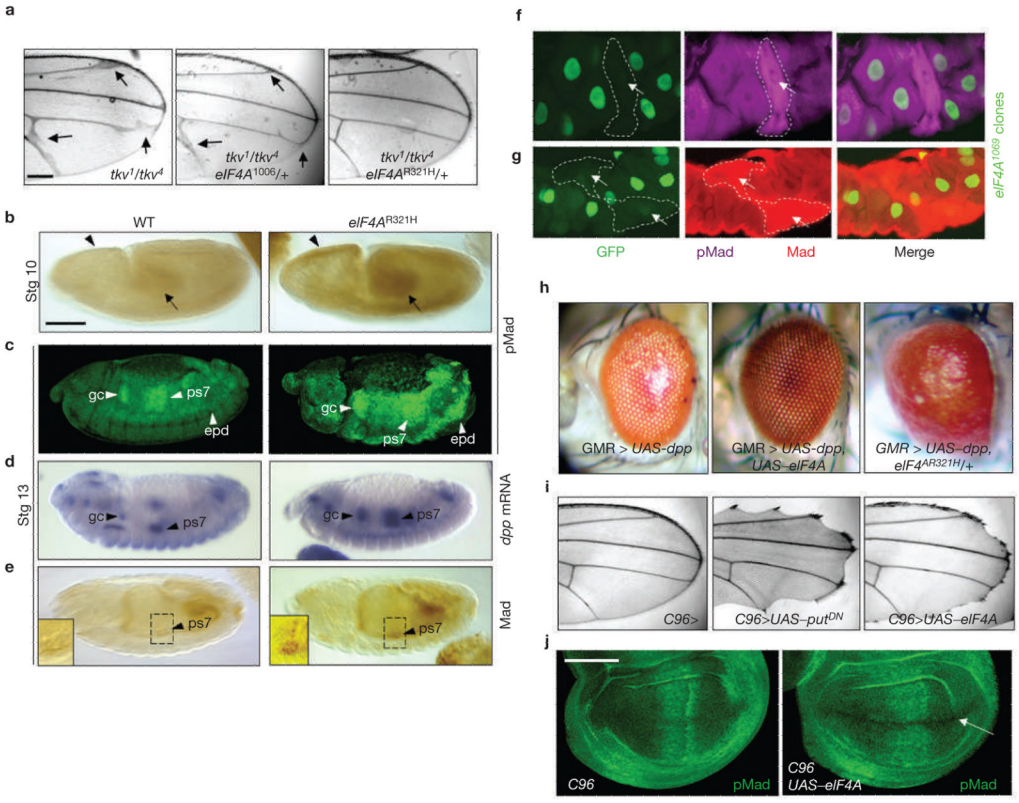

Figure 1.

Levels of eIF4A affect Dpp signalling and Mad protein levels. (a) Adult wings of different genotypes are shown anterior side up. Note the 'thick veins' (arrows) in the tkv^{1}/tkv^{4} wing and the suppression by $eIF4A^{1006}$ or $eIF4A^{R321H}$. (b–e) Whole-mount embryos stained with anti-pMad (brown in b, green in c), *dpp* antisense RNA (blue in d) and anti-Mad (brown in e) are shown anterior to the left and dorsal side up. (b) Higher levels of pMad signals in the dorsal epidermal cells (arrowhead) and posterior midgut (arrow) of stage 10 $eIF4A^{R321H}$ embryos (right) than in wild-type (WT) embryos (left). (c) At stage 13, pMad signals were detected in parasegment 7 (ps7), gastric caeca (gc) and the epidermis (epd) wild-type embryos (left). In $eIF4A^{R321H}$ embryos, pMad signals were detected at higher levels and expanded domains in all these tissues, such that pMad staining was seen in significantly larger areas of in gc and ps7 and broader spatial extent in the epidermis (right). (d) Increased *dpp* transcription is indicated by wider domains of *dpp* mRNA signals in gc and ps7 in $eIF4A^{R321H}$ embryos (right). (e) Little or no Mad protein is detected in ps7 of wild-type embryos (left), but is detected in discrete cells of ps7 of $eIF4A^{R321H}$ embryos (right). (f–g) Adult presumptive gut tissues of the 3rd instar larvae were doubly stained for GFP (green; marks nuclei of $eIF4A^{+}$ cells), and pMad (magenta in f) or Mad (red in g) are shown partially. Note that increased levels of pMad and Mad were detected within $eIF4A^{1069}$ mutant cells (lack of green nuclei). Arrows point to nuclei lacking GFP. (h) Expressing *dpp* by *GMR–Gal4* resulted in rough and bulging eyes (left), which was completely suppressed by coexpressing $eIF4A^{+}$ (centre). Expressing *dpp* by *GMR–Gal4* in a $eIF4A^{R321H}/+$ background resulted in lethality (4% viability; $n = 188$). A small number of survivors exhibited more severe roughness and outgrowth of eye tissues (right). (i) Expressing dominant-negative Put or eIF4A by the wing-margin-specific *C96–Gal4*. (j) Loss of pMad in wing-margin primordial cells (arrow) of the 3rd instar imaginal discs stained with anti-pMad (green). All scale bars equal 100 μm.

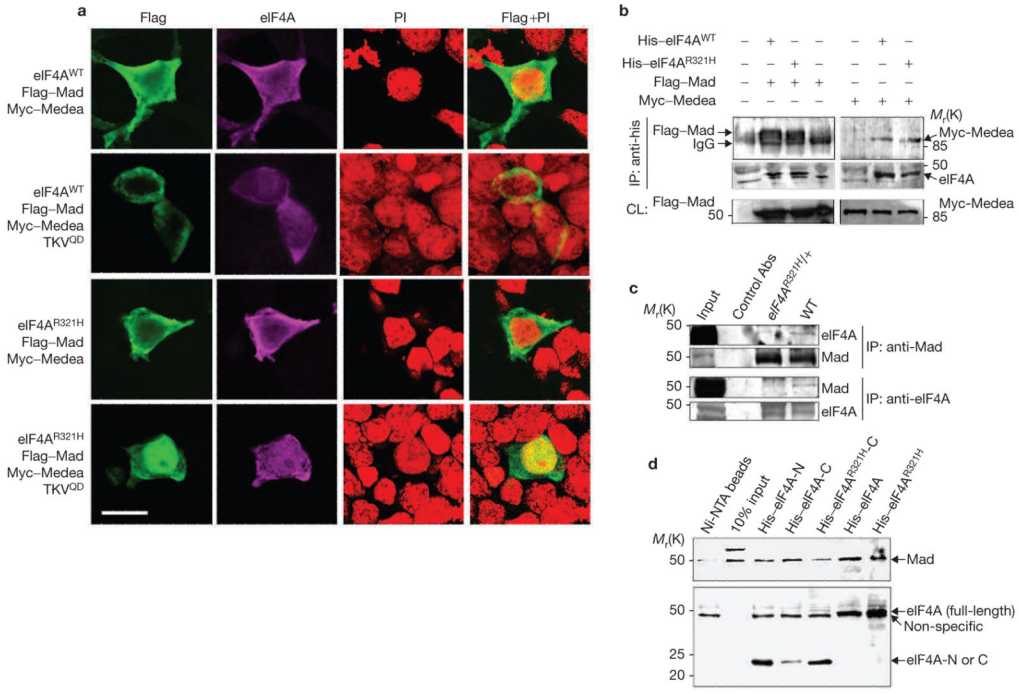

Figure 2.

Physical association of eIF4A with Mad and Medea. (a) Flag–Mad, Myc–Medea, and eIF4A^{WT} or eIF4A^{R321H} were co-transfected into 293T cells with or without Tkv^{QD}. Cells were stained with anti-Flag (green), anti-eIF4A (magenta) and propidium iodide (PI; red) to reveal the subcellular localization of transfected Mad and eIF4A. (b) 293T cells were co-transfected with Flag–Mad, Myc–Medea, eIF4A^{WT} and eIF4A^{R321H} in different combinations, as indicated. Cell lysates were immunoprecipitated (IP) with anti-His (for eIF4A), and the immunoprecipitates were subjected to SDS–PAGE and blotted with antibodies, as indicated. Note that co-immunoprecipitation of Mad and Medea with eIF4A occurred. (c) *Drosophila* embryo extracts from wild-type or *eIF4A^{R321H}* heterozygotes were immunoprecipitated with rabbit anti-eIF4A or goat anti-Mad, or with rabbit anti-βgal or goat anti-HA antibodies (negative controls, respectively), and the immunoprecipitates were subject to SDS–PAGE and blotted with indicated antibodies. (d) As the R321H mutation is located in the carboxy-terminal half of the eIF4A protein[1], which consists of substrate (RNA)-binding domains, the protein was divided into amino- and C-terminal halves, such that eIF4A^{WT} and eIF4A^{R321H} shared the same N-terminal fragment but different C-terminal fragments, with a different amino acid at position 321. His-tagged N-terminal, C-terminal, or full-length eIF4A^{WT} or eIF4A^{R321H} were expressed from *Escherichia coli*. The proteins were incubated with *Drosophila* embryo extracts and were then pulled down by Ni-NTA agarose beads, subjected to SDS–PAGE, and blotted with anti-Mad and anti-histidine. Note that Mad is pulled down by all species of eIF4A proteins, but in higher amounts by eIF4A^{WT} full-length (lane 6) and C terminus (lane 4). The anti-histidine antibody also recognizes a non-specific band that co-migrated with full-length eIF4A. For each binding assay above, the membrane was blotted with an antibody against the target protein of interest, and was then stripped of bound antibodies and re-blotted with an antibody against the bait protein. See Supplementary Information Fig. S5 for full-length gels.

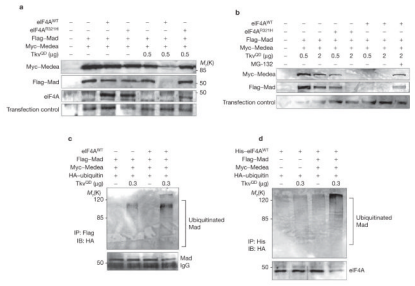

Figure 3.

eIF4A promotes Dpp signalling-dependent Mad and Medea degradation. (a–b) eIF4A induces Tkv^{QD}-dependent degradation of Mad and Medea. (a) 293T cells were transfected with Flag–Mad, Myc–Medea and $eIF4A^{WT}$ (or $eIF4A^{R321H}$) with or without low-level Tkv^{QD} (0.5 μg) in combinations, as indicated. Cell lysates were subject to SDS–PAGE and were blotted with anti-Flag, anti-Myc and anti-eIF4A consecutively. Note the apparent degradation of Medea, Mad and $eIF4A^{WT}$ in the presence of Tkv^{QD} (lane 6), whereas no degradation was detected in the absence of Tkv^{QD} (lanes 2–4) or $eIF4A^{WT}$ (lanes 5 and 7). (b) eIF4A-stimulated degradation depends on the proteosome. 293T cells were co-transfected with Flag–Mad, Myc–Medea, $eIF4A^{WT}$ (or $eIF4A^{R321H}$), and different amounts of Tkv^{QD}, and treated with the proteosome inhibitor MG-132, as indicated. Note the degradation of Medea and Mad in the presence of $eIF4A^{WT}$ and, to a lesser extent, $eIF4A^{R321H}$ at indicated Tkv^{QD} concentrations, which was inhibited by MG-132. (c) eIF4A promotes Tkv^{QD}-dependent ubiquitination of Mad. 293T cells were transfected with His–$eIF4A^{WT}$, Flag–Mad, Myc–Medea and HA–ubiquitin with or without low levels of Tkv^{QD} in the presence of MG-132. Mad was immunoprecipitated with anti-Flag and its ubiquitination was detected by anti-HA. Note the increased Mad ubiquitination in the presence of eIF4A (lane 4, compare with lane 2). (d) Ubiquitination of eIF4A depends on the presence of Mad, Medea and Tkv^{QD}. 293T cells were transfected, as indicated, without added MG-132. eIF4A was immunoprecipitated by anti-histidine and its ubiquitination was detected by anti-HA. Note the dramatic increase of ubiquitinated $eIF4A^{WT}$ in the presence of Mad, Medea and Tkv^{QD} (lane 4), compared with either lack of Mad and Medea (lane 2) or Tkv^{QD} (lane 3). See Supplementary Information Fig. S5 for full-length gels.

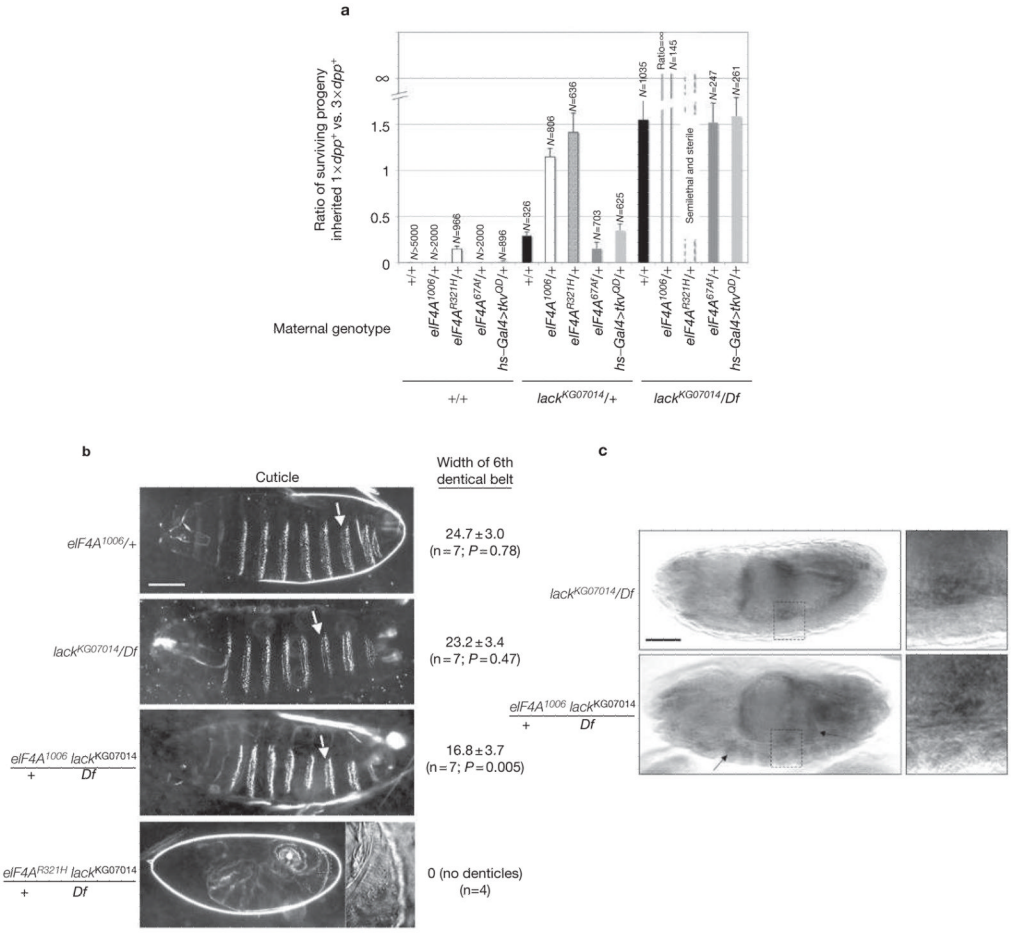

Figure 4.

eIF4A acts synergistically with and independently of DSmurf. (a) *eIF4A* mutations, but not those of *eIF4E* or activated TKV, interact synergistically with *DSmurf* mutations. The effects of maternal mutations on the viability of 1xdpp^+ versus 3xdpp^+ progeny are plotted as the ratios of these two categories. Females of the indicated genotypes were mated to 0xdpp^+/2xdpp^+ males. The F1 progeny would inherit either 1xdpp^+ or 3xdpp^+. Note the ratio is infinity (∞) for progeny of *eIF4A*^{1006}/+;*lack*^{KG07014}/Df mothers, and no progeny were produced by *eIF4A*^{R321H}/+;*lack*^{KG07014}/Df mothers. *Df = Df(2R)Exel7149*, which removes *DSmurf*. (b). *eIF4A* mutations further enhance the phenotypes of flies lacking maternal and zygotic DSmurf. The cuticles of embryos derived from females of the indicated genotype mated to *lack*^{KG07014}/Df males. Dorsalization was quantified by the number of denticles in the first row of the 6th ventral denticle belt (arrow). Note that embryos heterozygous for *eIF4A*^{1006} or *eIF4A*^{R321H} and maternally and zygotically null for DSmurf exhibited narrower or no ventral denticle belts, respectively. Inset, high magnification of boxed area showing dorsal hairs. *eIF4A*^{R321H}/+;*lack/Df* females are sterile. They lay very few eggs, most of which seem to be unfertilized (white eggs with no cuticles), regardless to which males they were mated. However, a small percentage (<5%) of the eggs appeared to be fertilized and secreted cuticles. These eggs are completely dorsalized (bottom panel). (c). Mutations in eIF4A further increase Mad protein accumulation in *lack/Df* embryos. Stage 13 embryos of the indicated genotypes were stained by anti-Mad (dark stains). Note that *lack/Df* embryos exhibited elevated levels of Mad protein compared with the wild type, similar to *eIF4A*^{R321H}/+ embryos (compare with Fig. 1e), and

eIF4A^{1006}*/+;lack/Df* embryos accumulate Mad protein in even more cells, such as in the germ bands and guts (arrows). Right panels are higher magnifications of the boxed area (ps7). Scale bar, 100 μm.

Table 1

Mutations in *eIF4A* augment Dpp signalling

Genotype	Viability *(n)*	Egg hatching rate *(n)*	Phenotype
Mad sax^{1}/+	100%	0% (209)	Eggs weakly ventralized
Mad sax^{1}/eIF4A^{1006}	100%	24% (195)	Eggs normal
Mad sax^{1}/eIF4A^{R321H}	100%	95% (187)	Eggs normal
tkv^{1}/tkv^{4}	23% (230)	ND	Wing veins thickened
tkv^{1}/tkv^{4} eIF4A^{1006}	94% (304)	ND	Minor wing-vein defects
tkv^{1}/tkv^{4} eIF4A^{R321H}	101% (226)	ND	Wing veins normal
hs–Gal4/+;UAS–dpp/+ (plus heat-shock)	98% (203)	ND	Ectopic wing veins
hs–Gal4/+; eIF4A^{R321H}/+; UAS–dpp/+ (plus heat-shock)	0% (349)	ND	Lethality
hs–Gal4/+; UAS–eIF4A/+; UAS–dpp/+ (plus heat-shock)	100% (128)	ND	Wing veins normal

The viability of flies of a particular genotype was determined by comparing with siblings from the same cross from which they were derived. The egg hatching rate was calculated for eggs produced by viable females of the indicated genotypes that were mated with wild-type males. Percentage viability was calculated by comparing with siblings without inherited *eIF4A* mutations or transgenes from the same cross. *n* indicates the number of embryos or adult flies examined. ND, not determined. Heat-shock was administered by incubating pupae at 37 °C for 30 min at 18 h after puparium formation.